Low Noise Ultrashort Pulse Generation by Direct RF Modulation at 22 GHz from an AlGaInAs Multiple Quantum-Well Laser at 1.55 μm

Edris Sarailou, Abhijeet Ardey, *Student Member, IEEE*, and Peter J. Delfyett, *Fellow, IEEE*

***Abstract*— We report subpicosecond pulse generation at 22 GHz from a two-section passively mode-locked laser at 1.55 μm, using a novel AlGaInAs quantum-well wafer. By carefully designing the metal pad and the isolation layer, we are able to hybridly mode-lock the laser by modulating the saturable absorber at the fundamental repetition rate and thus achieve a low timing jitter of ∼280 fs (1 Hz–100 MHz).**

***Index Terms*— AlGaInAs, clock synchronization, hybrid mode-locking, laser noise, mode-locked (ML) laser.**

I. Introduction

MONOLITHIC high-repetition-rate lasers have drawn considerable attention for applications in photonic analog-to-digital conversion, clock recovery and arbitrary waveform generation [1]–[3]. These compact and monolithic sources generate subpicosecond pulses at high repetition rates but exhibit large timing jitter due to amplified spontaneous emission (ASE) and lack of external stabilization. In order to realize a low noise mode-locked laser (MLL) by synchronizing to an external clock at high frequencies (> 20 GHz), several methods such as subharmonic hybrid mode-locking (SHML) [4], fundamental hybrid mode-locking (FHML) using semi-insulating substrate [5] and optical synchronous mode-locking [6] have been presented. The first of the above methods overcomes the shallow radio frequency (RF) modulation issue at high frequencies but introduces unwanted amplitude modulation and excess timing jitter. The second requires a semi-insulating wafer and lengthy fabrication process while the third typically involves injection of a low noise mode-locked laser into the laser cavity, requiring an additional laser.

A promising new AlGaInAs-InP strained quantum well (QW) material at 1.55-μm has recently been used to fabricate MLLs [7]. This material system is beginning to replace conventional InGaAsP-InP materials owing to a larger conduction band discontinuity ($\Delta E_c = 0.72\ \Delta E_g$) and a smaller valence band discontinuity. The former enables uncooled operation over a large dc bias range and the latter enables a large range of reverse bias voltage, allowing for shorter pulse durations [7].

In this letter, we present 860 fs pulses from a monolithic AlGaInAs multiple quantum well two-section MLL fabricated by employing a very simple self-aligned wet etching technique. By using Benzocyclobutene (BCB) as the isolation layer (1.3-μm-thick) and minimizing the metal pad size, we were able to modulate the saturable absorber (SA) at 22 GHz and synchronize the laser to an external source. By doing so we achieved very effective FHML (280 fs timing jitter) which shows distinct advantages over other methods.

II. Device Structure and Fabrication

The epitaxial structure of the wafer is grown on a sulfur-doped InP substrate by metal organic vapor phase epitaxy (MOVPE). The active region consists of five 6-nm-thick AlGaInAs compressively strained wells showing photoluminescence at 1.54 μm and six 10-nm-thick AlGaInAs barriers. These wells and barriers are sandwiched between 60-nm-thick AlGaInAs layers which serve as the separate confinement hetrostructure (SCH). The active region is protected by a (1.1Q) InGaAsP wet etch stop layer followed by 1.6-μm-thick p-type InP upper cladding. Electron injection is facilitated by having 50 nm of (1.3Q) InGaAsP and 200 nm of heavily Zn-doped (1.5e19 cm^{-3}) InGaAs layer. The fabrication process starts by depositing 200 nm of Si_3N_4 via plasma-enhanced chemical vapor deposition (PECVD). The 2.4-μm-width ridge waveguides are defined using the standard positive photolithography followed by CF_4:O_2 (12:1) reactive ion etching (RIE) to transfer the patterns to the Si_3N_4. The first two heavily-doped layers are removed in one step wet etching using H_2SO_4:H_2O_2:H_2O (1:1:10). The InP cladding layer is subsequently removed using HCl:H_3PO_4 (1:1) etchant stopping selectively at the top of the waveguiding layer. After removing the Si_3N_4 masking layer, a 3.5-μm-thick BCB polymer layer is spin-coated for electrical isolation. Curing the BCB at 250 °C for one hour is followed by etching it down uniformly using CF_4:O_2 (1:2) based RIE to expose the waveguide by 300 nm. The p-metal (Ti-5/Au-300 nm) is deposited using an e-beam evaporator after standard negative photolithography. Resist lift-off is followed by the rapid thermal annealing (RTA) at 430 °C for 30 seconds. The electrical isolation between the gain section and SA is

Manuscript received March 27, 2012; revised June 16, 2012; accepted July 10, 2012. Date of publication July 31, 2012; date of current version August 10, 2012. This work was supported in part by the Army Research Office Contract W911NF-10-1-0189.

The authors are with CREOL, The College of Optics and Photonics, University of Central Florida, Orlando, FL 32816 USA (e-mail: esarailo@creol.ucf.edu; aardey@creol.ucf.edu; delfyett@creol.ucf.edu).

Color versions of one or more of the figures in this letter are available online at http://ieeexplore.ieee.org.

Digital Object Identifier 10.1109/LPT.2012.2208738

achieved by removing the first two heavily-doped layers by H_2SO_4:H_2O_2:H_2O wet etchant. This provides us with a 3 kΩ resistance for the 10-μm gap. The fabrication is concluded by lapping and polishing the wafer to 150 μm thickness and depositing the n-metal (Ni-2/Ge-20/Au-200 nm) and RTA. The laser bar is cleaved to a total length of 1912 μm with a 56 μm SA. Fig. 1 shows the waveguide structure and the contact layout. The facets are uncoated and the laser is mounted with the epi layer up on a copper stud connected to a thermo-electric cooler (TEC) to maintain the temperature at 20 °C.

III. Experimental Results

Passive mode-locking is achieved by forward biasing the gain section using a simple dc probe and by reverse biasing the SA. With the help of an 18 GHz bias tee and a 40 GHz ground-signal (GS) microwave coplanar probe, the reverse bias voltage and the RF signal are applied to the device. Here the signal and ground probes were connected to the SA and the gain section respectively as shown in Fig. 1. Fig. 2(a) shows the typical output power-current characteristics for different reverse bias SA voltages. From this figure a threshold current of 57 mA is obtained for the unbiased SA, and it increases as the reverse bias voltage is increased. Output light is coupled to a single mode fiber using an aspheric lens and a free space isolator is used to avoid any back reflection. A fiberized optical semiconductor amplifier is used to amplify the output light.

Stable passive mode-locking is observed for bias current values of 75 mA to 140 mA with reverse bias voltages of -2 V to -3.9 V. Fig. 2(b) shows the optical spectrum of the passively MLL running at 123 mA and reverse bias voltage of -3.9 V which gave us the shortest optical pulse. The optical spectrum centered at 1548 nm has a 3-dB bandwidth of 9.8 nm. Fig. 2(c) shows the corresponding RF spectrum at 22.14 GHz and its harmonic detected by a 33 GHz fast InGaAs PIN photodetector and observed by a 50 GHz RF spectrum analyzer. Maintaining a constant temperature, the pulse repetition rate can be tuned by about 400 MHz by changing the biasing current and the reverse bias voltage. Fig. 2(d) shows the optical intensity autocorrelation of the isolated pulse obtained by the second-harmonic autocorrelator. The autocorrelation signal of the pulse is equal to 1.31 ps which deconvolves to 860 fs by using 0.656 as the deconvolving factor obtained from simulation. The simulation is done using the optical power spectrum and assuming flat spectral phase. The results imply a time-bandwidth product of 1.05 which is 2.6 times transform-limited.

We minimized the capacitance by reducing the size of the SA metal pad to 56 μm$\times$100 μm. By having the 1.3-μm-thick BCB layer as an insulating layer further helped to reduce the capacitance of SA pad. Careful design of these parameters enabled us to drive the SA at very high frequencies (>20 GHz) very effectively without the need for semi-insulating substrate wafers that require more fabrication processes [5].

Hybrid mode-locking is achieved by using a low noise RF synthesizer (Agilent E8254A) to drive the two-section MLL. SMA cables are used to transmit the RF signal and a 20-dB

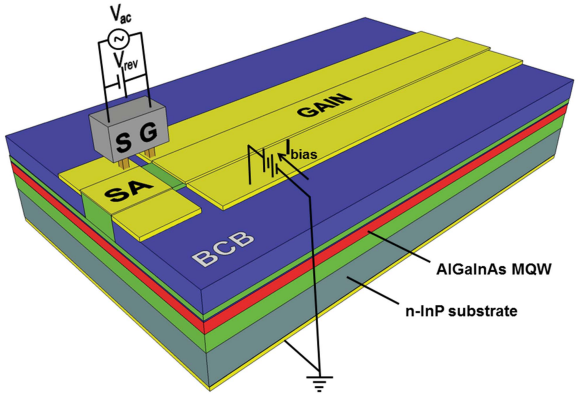

Fig. 1. Device schematic showing the waveguide structure and contact layout.

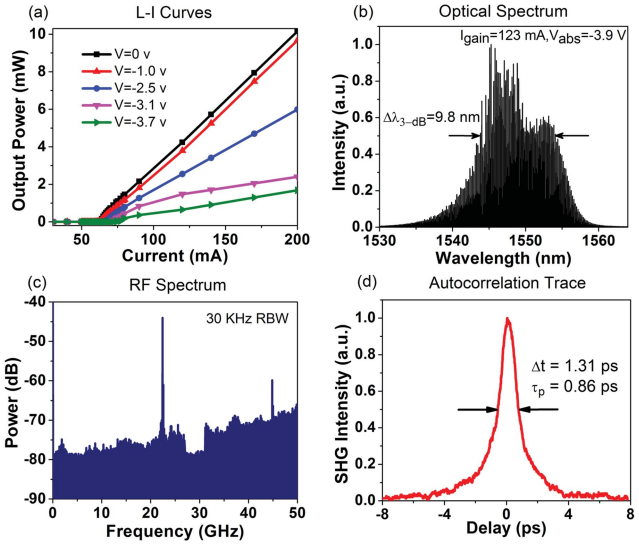

Fig. 2. (a) Typical output power-current characterization of the two-section MLL at 20 °C for different reverse bias voltages, (b) optical spectrum of the mode-locked laser for shortest pulse at I_{gain} = 123 mA and V_{abs} = -3.9 V, (c) corresponding RF spectrum, and (d) autocorrelation trace of the isolated pulse under passive mode-locking.

RF amplifier is used to compensate the huge loss of these cables and the losses introduced by the 18 GHz bandwidth bias tee and other connectors. Fig. 3 shows the double side band noise spectrum for the device running in the passive and fundamental hybrid and sub-harmonic hybrid mode-locked (n = 2) regimes respectively. The bias current and the reverse bias voltage are 80 mA and -3.1 V respectively. The applied RF is tuned to 22.417783 GHz to minimize the pedestal. On applying the RF signal, the RF tone linewidth is seen to decrease from 1.5 MHz to sub Hz. As seen in Fig. 3, by increasing the RF power, the RF noise is drastically reduced (more than 20 dB decrease is observed by applying 15 dBm RF signal). Fig. 3 (inset) shows the amplified laser output time domain traces with 44.6 ps period using a 50 GHz Agilent sampling scope triggered by 1.868148583 GHz signal using another RF synthesizer. The RF synthesizers and RF spectrum analyzer used are synchronized to each other. Because of the frequency response of the photodetector and cables, only

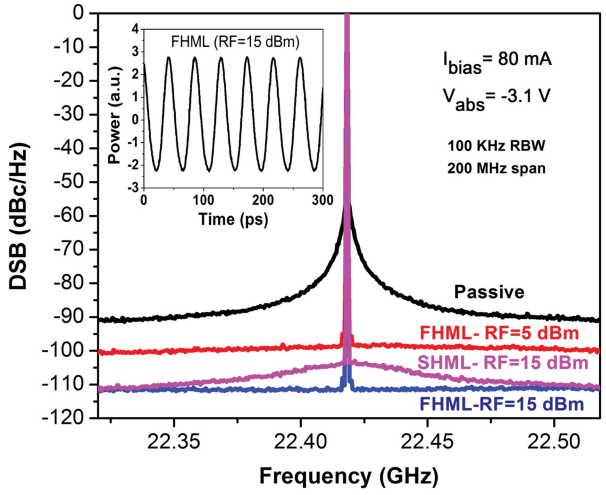

Fig. 3. Double-side band noise spectrum for passive FHML at different RF powers and SHML (n = 2). Inset: sampling scope trace for the FHML at an RF power of 15 dBm.

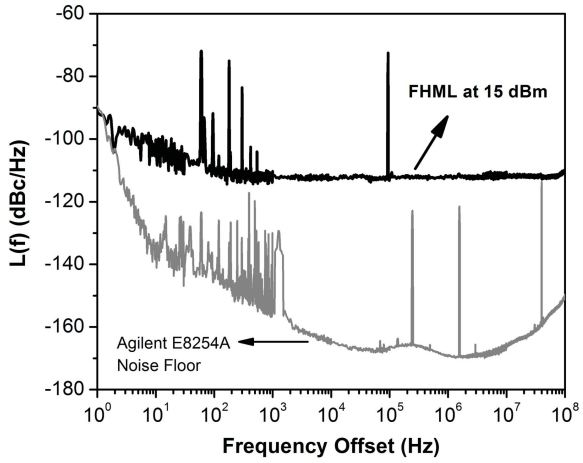

Fig. 4. Residual phase noise power spectral density of the FHML laser (black) under $I_{gain} = 80$ mA, $V_{abs} = -3.1$ V, and the RF power of 15 dBm. Also shown is the noise floor of the measurement (grey).

the first harmonic is observed. For comparison SHML was also performed on the device with 15 dBm RF power and by small tuning of the modulation frequency to have the minimum pedestal. As can be seen in Fig. 3, SHML has much higher RF noise validating the effectiveness of our approach. Fig. 4 shows the residual phase noise power spectral density of the mode-locked laser under 15 dBm RF power, along with the noise floor of the measurement system, measured by a HP 70420A carrier noise test set and normalized to a 1 Hz Resolution bandwidth. From this data the timing jitter for the 1 Hz-100 MHz range is calculated to be 280 fs.

IV. Conclusion

In this letter, we demonstrated a simple self-aligned wet etching process to fabricate AlGaInAs quantum well MLLs. This material system has shown distinct advantages compared to the conventional InGaAsP-InP system. Pulses of 860 fs were obtained at a high repetition rate of 22 GHz. By carefully designing the metal pads, and by having 1.3-μm-thick layer of BCB as the insulation layer, very effective RF modulation of the SA was made possible at the round-trip of the cavity. Low timing jitter of 280 fs (1 Hz-100 MHz) at the fundamental repetition rate was achieved. These results confirm the potential of the novel, simple and cost-effective laser design as a compact source of low noise high repetition rate optical pulses.

References

[1] A. S. Bhushan, F. Coppinger, and B. Jalali, "Time-stretched analog-to-digital conversion," *Electron. Lett.*, vol. 34, no. 9, pp. 839–840, 1998.

[2] J. Chou, Y. Han, and B. Jalali, "Adaptive RF-photonic arbitrary waveform generator," *IEEE Photon. Technol. Lett.*, vol. 15, no. 4, pp. 581–583, Apr. 2003.

[3] P. J. Delfyett, I. Ozdur, N. Hoghooghi, M. Akbulut, J. Davila-Rodriguez, and S. Bhooplapur, "Advanced ultrafast technologies based on optical frequency combs," *IEEE J. Sel. Topics Quantum Electron.*, vol. 18, no. 1, pp. 258–274, Jan.–Feb. 2012.

[4] C. Ji, *et al.*, "Electrical subharmonic hybrid mode locking of a colliding pulse mode-locked laser at 28 GHz," *IEEE Photon. Technol. Lett.*, vol. 17, no. 7, pp. 1381–1383, Jul. 2005.

[5] H. K. Lee, *et al.*, "Efficient direct locking of colliding pulse mode-locked lasers on semi-insulating substrate at 1.5 μm," *IEEE Photon. Technol. Lett.*, vol. 14, no. 8, pp. 1049–1051, Aug. 2002.

[6] H. Kurita, T. Shimuzu, and H. Yokoyama, "Experimental investigations of harmonic synchronization conditions and mechanisms of mode-locked laser diodes induced by optical-pulse injection," *IEEE J. Sel. Topics Quantum Electron.*, vol. 2, no. 3, pp. 508–513, Sep. 1996.

[7] L. Hou, *et al.*, "Subpicosecond pulse generation at quasi-40-GHz using a passively mode locked AlGaInAs-InP 1.55 μm strained quantum well laser," *IEEE Photon. Technol. Lett.*, vol. 21, no. 23, pp. 1731–1733, Dec. 1, 2009.